JOURNAL OF GEOPHYSICAL RESEARCH, VOL. 106, NO. D7, PAGES 7375–7385, APRIL 16, 2001

# Joint statistics of photon path length and cloud optical depth: Case studies

Qilong Min and Lee C. Harrison

Atmospheric Sciences Research Center, The State University of New York at Albany

Eugene E. Clothiaux

Department of Meteorology, The Pennsylvania State University, University Park

**Abstract.** We show the joint statistics of photon path length and cloud optical depth for cloudy sky cases observed at the Atmospheric Radiation Measurement (ARM) Southern Great Plains (SGP) site between September and December 1997. The photon path lengths are retrieved from moderate resolution oxygen A-band observations taken by a rotating shadow band spectroradiometer (RSS). For high optical depth cloud cases, two different populations in the scattergram of the path length versus cloud optical depth are apparent. One population is a result of single-layer cloud cases that exhibit a small variation of path length enhancement over a large optical depth range, together with a strong correlation between the radiation field and the cloud liquid water path, while the second population is attributed to multiple-layer cloud cases with large variability of enhanced photon path lengths. When the optical depth is less than 5, the population of cases appears to bifurcate as the solar air mass increases, with the lower branch exhibiting pressure-weighted path lengths shorter than the direct beam path lengths at these larger solar zenith angles. Using information from a millimeter-wave cloud radar, together with lidar and balloon-borne sonde data to further analyze these cases demonstrates that this bifurcation is caused by the altitude of the scattering; thin clouds aloft produce the lower branch and low-level aerosols produce the upper branch.

## 1. Introduction

All problems that require a realistic account of the effects of radiation in a cloudy atmosphere must be concerned with the spatial and temporal variability of clouds and the impact of this variability on the radiative processes of interest. Many studies have shown the sensitivity of cloud radiative properties to cloud spatial structure [*Stephens,* 1976; *Welch and Wielicki,* 1986; *Stephens,* 1988a, 1988b; *Cahalan and Snider,* 1989; *Lovejoy et al.,* 1993; *Cahalan et al.,* 1994a, 1994b; *Marshak et al.,* 1995; *Davis et al.,* 1996; *Marshak et al.,* 1997; *Davis et al.,* 1997]. *Stephens* [1988a, 1988b] uses a general full matrix solution of the discretized three-dimensional radiative transfer equation to demonstrate that the domain-averaged radiative properties of a heterogeneous atmosphere depend not only on the averaged optical properties but also on the horizontal distribution of these properties within the layer, and the effect of multiple scattering on the transfer of radiation through a heterogeneous atmosphere is to filter out smaller-scale structures leaving the radiance dependent only on the grossest scales. *Cahalan and Snider* [1989] found that spatial wavenumber spectra $E(k)$ for Landsat radiance fields approximate a power law with an exponent $\beta \approx 5/3$ over a subrange of $k$, which follows the wavenumber spectra of vertically integrated liquid water path (LWP) from ground-based microwave radiometers; and at scales smaller than some critical scale, generally around 0.2 - 0.4 km, the Landsat power spectra become much steeper with $\beta > 3$. This study on scale invariance and radiative smoothing has been expanded in a variety of ways by their group [*Marshak et al.,* 1995; *Davis et al.,* 1996; *Marshak et al.,* 1997; *Davis et al.,* 1997]. These subsequent studies are primarily on a small-scale upwelling radiance which are relevant to remote sensing.

Efforts to understand radiation transfer through inhomogeneous cloud systems and current concerns in atmospheric radiation modeling about potential anomalous cloud absorption [*Cess et al.,* 1995] have revived interest both in modeling approaches that explicitly use a path length distribution function and in methods by which such distributions can be measured [*Grechko et. al.,* 1973; *Harrison and Min,* 1997; *Pfeilsticker et al.,* 1998; *Veitel et al.,* 1998; *Min and Harrison,* 1999;



Paper number 2000JD900490.
0148-0227/01/2000JD900490$09.00

*Stephens and Heidinger,* 2000; *Heidinger and Stephens,* 2000]. The scattering properties of clouds and aerosols vary slowly with wavelength; the principle of equivalence then allows conclusions about the radiative properties of the atmosphere at disparate wavelengths to be made from a photon path length distribution measurement in one wavelength band [*van de Hulst,* 1980].

Direct measurements of path length distributions would allow correct radiative transfer calculations, constrain or perhaps resolve cloud anomalous absorption, and most importantly act as a data set against which General Circulation Model (GCM) cloud diagnostic parameterizations could be tested for fidelity to real atmospheres. In addition, since photon transport in inhomogeneous media is inherently a random and statistical process, the photon path length distribution, as a statistical quantity, may be of value in a broad range of atmospheric radiative transfer studies.

*Min and Harrison* [1999] used routine measurements of the rotating shadow band spectroradiometer (RSS) in the $O_2$ A-band to retrieve a mean photon path length. Using their retrieval algorithm of cloud optical depths and mean droplet radii from multifilter rotating shadowband radiometer (MFRSR) data [*Min and Harrison,* 1996], we also studied the joint statistics of photon path length and cloud optical properties at the ARM SGP site from September to December 1997, demonstrating that information derived from photon path lengths allows diagnostics of sky homogeneity and constrains models of radiation transfer in cloudy skies.

Here we extend the *Min and Harrison* [1999] study by examining high time resolution data streams from colocated instruments at the ARM SGP site, including broadband and narrowband radiometers, a microwave radiometer, ballon-borne soundings, a millimeter-wave cloud radar, a micropulse lidar, a ceilometer, and other relevant instruments. We focus on the large-scale fluxes and transmittances that are the important quantities for cloud overlap schemes and sub-grid-scale parameterizations in GCMs.

## 2. Measurements and Methodology

### 2.1. Cloud Optical Depth and Mean Photon Path length

With surface measurements of spectral irradiance from either a MFRSR or RSS, and total liquid water path (LWP) from a microwave radiometer (MWR), we simultaneously retrieve the cloud optical depth $\tau$ and the effective radius $r_e$ of the cloud droplets through the use of a nonlinear least squares minimization in conjunction with an adjoint method of radiative transfer [*Min and Harrison,* 1996]. In this study we use spectral irradiance measurements of a MFRSR for retrievals of cloud optical properties, since the sampling interval of 20 s is the same as for the liquid water and water vapor path measurements of a zenith-viewing MWR. (The RSS and MMCR take data every 60 s.) In all the following results, optical depths greater than 5 are determined from the above retrieval algorithm using the total horizontal transmittance at 415 nm from a MFRSR. Below optical depths of 5 the retrieval is based on Beer's law using direct-beam extinction at 415 nm.

The RSS [*Harrison et al.,* 1999] is a CCD-array spectrograph coupled to an irradiance foreoptic. It uses an automated shadow-banding technique to provide spectrally resolved direct-normal, diffuse-horizontal, and total-horizontal irradiances, where the passbands and responsivities are guaranteed to be identical for the separated spectral irradiance components. For our purposes the measurements of the direct solar beam under clear skies allow accurate calibration of a retrieval for a mean photon path length from oxygen A-band spectroscopy. Our retrieval algorithm for this from RSS data is described by *Min and Harrison* [1999]. We will not repeat the details but provide an overview and definition of terms, so we hope the following discussion of observations are understandable.

The lines in the A-band are in two branches with individual lines well fitted as Lorentzian in the lower atmosphere. In both branches the lines at low rotational quantum numbers are very "strong" with centerline transmissions as low as $10^{-40}$ when observed at the Earth's surface. With the modest resolution of the RSS ($\approx 40\,\mathrm{cm}^{-1}$) we do not resolve the two branches of the band and are far from the resolution needed to see details of an individual lineshape. The RSS resolution is adequate to see "the center" of the band as distinct from the wings to either side, which are the lines with higher rotational quantum numbers. The lines in the wings of the band appear "weak" because at atmospheric temperature few of the oxygen molecules populate these higher rotational states; consequently, the apparent strengths of the lines in the wings of the band are strongly temperature dependent due to Boltzman statistics of the populations.

$$k_i = \frac{S_i}{\pi}\frac{\alpha_i}{(\nu-\nu_i)^2+\alpha_i^2}, \tag{1}$$

where

$$\alpha_i = \alpha_i^0 \frac{p}{p_0}\left(\frac{T_0}{T}\right)^{1/2}, \tag{2}$$

$$S_i = S_i(T_0)\frac{T_0}{T}\exp^{[1.439E''(\frac{1}{T_0}-\frac{1}{T})]}. \tag{3}$$

$S_i$ is the line intensity, $\nu_i$ is the line-center wavenumber, and $\alpha_i$ is the line width for the $i$th line. $T_0$ and $p_0$ are standard temperature and pressure, respectively. $E''$ is the energy of the lower state of the transition, which increases significantly from the band center toward the wing region, while the normalized line strengths $S(T_0)$ decrease.

Our observations are dominated by the "strong" low-rotational-state lines at the center of the band. Their opacities are so large that essentially, no light is received

from the domains near line centers. The $E$" coefficents for these lines do not vary markedly (in contrast to the high rotational state lines). Hence in approximation we naturally sense the integral of the $O_2$ path length distribution weighted by $p/T^{3/2}$ from the equation in the Lorentzian when $|\nu - \nu_i| >> \alpha_i$.

In principle some information about the distribution of path length with pressure (altitude) could be obtained by very high resolution ground-based spectroscopy of the higher-rotational-state lines, but so far as we know, this has not yet been demonstrated. Similarly wing-to-center transmittance ratios, or the observation of the magnitudes of individual wing lines (which would not require the extreme resolution needed to accurately observe the line shape near its center), could yield some partition of path length versus temperature (an indirect surrogate for altitude), but we do not pursue this here.

To avoid uncertainties associated with absolute calibrations, we selected a pixel in the RSS spectrum from outside the oxygen A-band (near 751 nm) as a denominator and take ratios of the pixels inside the A-band to this pixel. We calibrate a transmittance model for each pixel from observed clear-sky direct-beam ratios. As discussed previously, diffuse-horizontal and direct-normal components measured by the RSS share the same instrument calibration. Hence we can apply these path length calibrations developed from direct-beam measurements (where the path length distribution is a known Dirac delta function) for retrievals of the mean photon path length in arbitary scattering atmospheres, given the understanding that it is moment-weighted by pressure and temperature as above.

In this study we usually show the mean incremental photon path length, defined as the difference between the mean photon path length through the atmosphere to the detector minus the direct-beam path length for the instantaneous solar zenith angle. This incremental path length is the path length effect of the scatterering in the atmosphere.

The units for mean incremental photon path lengths used here are air masses, (approximately secant (solar zenith angle)). Mean incremental photon path lengths can be negative if the pressure- and temperature-weighted photon path lengths are, on average, less than what would be observed in a clear-sky environment. As we will show, this circumstance prevails for optically thin clouds aloft at greater solar zenith angles.

### 2.2. Cloud Geometry and Wavenumber Spectrum

The ARM SGP site has been heavily instrumented to study clouds and radiation transfer. Cloud base height is measured by both a Belfort laser ceilometer (BLC) and a micropulse lidar (MPL). The resolution of the BLC is 7.6 m with an operational range from 15 m to approximately 5000 m above the ground. The MPL has a detection range up to 20 km with a resolution of 300 m. Consequently, the BLC data are used to monitor the cloud base height of low clouds, while MPL data are used to locate clouds aloft. Multiple cloud layers are derived from the millimeter-wave cloud radar (MMCR), a zenith-pointing 35-GHz radar, and from relative humidity profiles measured by a balloon-borne sounding system (BBSS) which launches rawinsondes at least 4 times a day. The cloud LWP measured from a MWR is an important quantity that records the temporal variability of cloud liquid water at the site.

For a realistic radiative transfer calculation it is important to consider the spatial (and temporal) variability of clouds, which are discarded in our usual plane-parallel assumptions. Scale-by-scale statistical analysis, such as wavenumber spectrum $E(k)$, is used here to characterize the cloud morphology, to study the physical processes that govern the variability at different scales, and to understand the relationship among the photon path length, radiation field, and cloud geometry.

For each overcast case, when the direct beam is fully blocked by clouds for the entire day, we compute the power spectrum by performing a FFT on both the LWP and the transmittance at 415 nm from a MFRSR for the frequency range less than 0.5/20 s, which is the Nyquist frequency for data sets with a sampling interval of 20 s. The wind speed and direction measured on a 10 m tower, as well as wind profiles measured by the BBSS over the ARM SGP site, indicate quite large variations in the wind fields from one case to the next. Temporal variations at the observation point are assumed to be primarily due to the advection of the spatial pattern, rather than to the local time dependence of a field [*Cahalan and Snider*, 1989]. Therefore we use the relation $v = \lambda f$, where $v$ is the advection speed and $\lambda$ is the wavelength, which are related to the wavenumber $k$ by $k = 2\pi/\lambda = 2\pi f/v$. With this transformation wavenumber has the physical unit of inverse length, $km^{-1}$. However, we have no measurement of wind velocities at cloud height beyond infrequent soundings. We use the averaged wind speed over a cloud layer from sounding profiles as the advection speed of a cloud system. Then in wavenumber space, we study the statistical information on a scale-by-scale basis.

## 3. Thin Cloud and Aerosol Cases

Joint statistics of photon path length and cloud optical depth presented by *Min and Harrison* [1999] show that populations of incremental path lengths (equal to total path length minus direct-beam path length) for optical depths greater than 5 appear to bifurcate as the solar zenith angle increases, with the lower branch exhibiting negative incremental path lengths for the greater solar air masses. Here we show three cases in which we correlate joint statistics with radar measurements to settle our speculation: the lower branch is

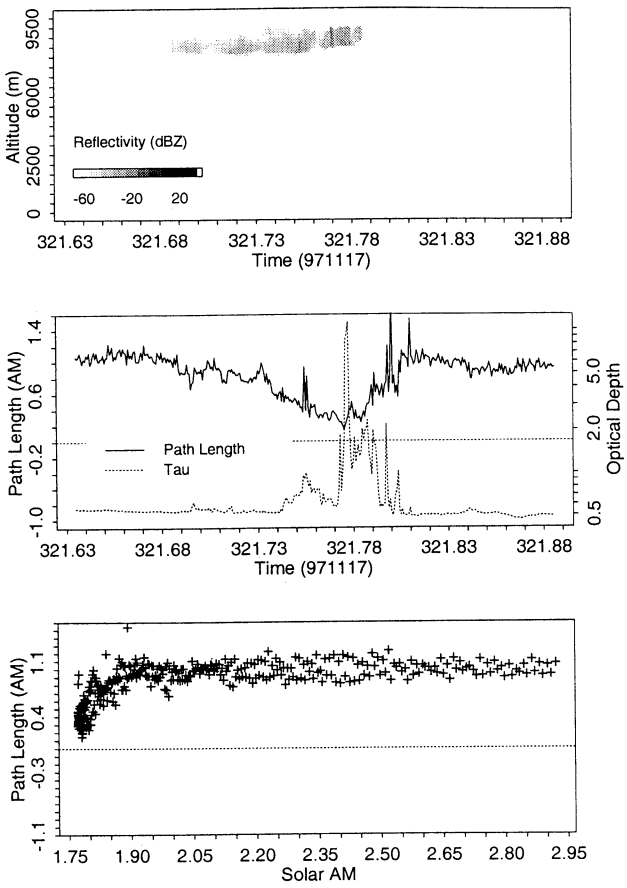


**Figure 1.** An aerosol and aloft thin cloud case on November 17, 1997. The top panel of the figure is the image of (MMCR) reflectivity, the middle panel shows the incremental path length inferred from the (RSS) and total optical depth derived from the (MFRSR), and the bottom panel shows the incremental path length versus solar air mass.

caused by thin clouds aloft and the upper branch by low-level aerosols.

### 3.1. Case 1 (Thin Cirrus Layer, November 17, 1997)

The top panel in Figure 1 shows the image of MMCR reflectivity on a day at the SGP site when high-altitude cirrus clouds appeared in the middle of the day with scattered low clouds. Both morning and afternoon periods were clear with relatively small variations of aerosol optical depth about a value of 0.29 at 415 nm. For the cirrus clouds at a mean altitude of about 8.6 km, optical depths varied from 0.3 to 1.5. Low clouds around 321.78 Julian time were located at 1.4 km with optical depths up to 10. The middle panel of Figure 1 shows the time series of mean incremental photon path length and total optical depth, while the bottom panel plots incremental path length versus solar air mass.

In the case of a single-low-level-scattering layer the cumulative path length down to the layer is nearly the direct-beam path length to the surface (Rayleigh scattering is low at 760 nm). Once scattered in the layer, a significant fraction of the photons travel long slant paths to the detector through the lower atmosphere, substantially increasing the incremental path length. As shown in Figure 1, the incremental path length of the diffuse sky when clouds are not present is nearly invariant over a large change of solar zenith angle, with a mean of 0.96 air masses.

When the scattering sources are at a high altitude (e.g., midday cirrus clouds), a fraction of the photons are scattered downward to the diffuser, resulting in shorter path lengths when the solar zenith angle is significantly greater than zero. The middle panel of Figure 1 illustrates that the incremental path length is reduced when clouds progress over the RSS. The large spikes appearing in the incremental path length plot may be due to inhomogenous cloud effects, as some photons bounce between clouds.

### 3.2. Case 2 (High Broken Cloud Layer, November 4, 1997)

The case shown in Figure 2 is quite different from the first case: high clouds occur in the morning and afternoon with altitudes above 4.3 km. In the clear-sky interval in the middle of the day, aerosol optical depths are low, 0.05 at 415 nm. During the clear-sky period

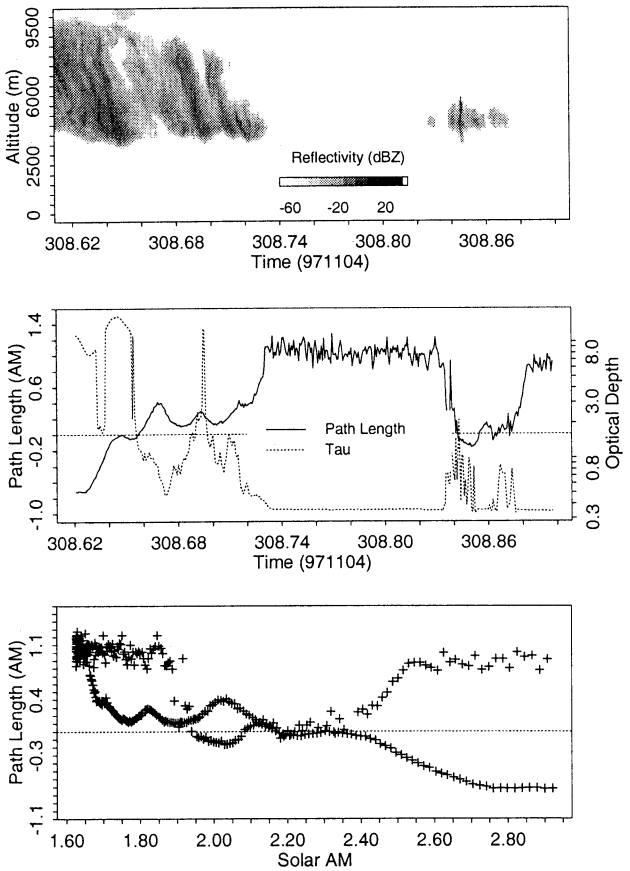


**Figure 2.** Same as in Figure 1 but for November 4, 1997.

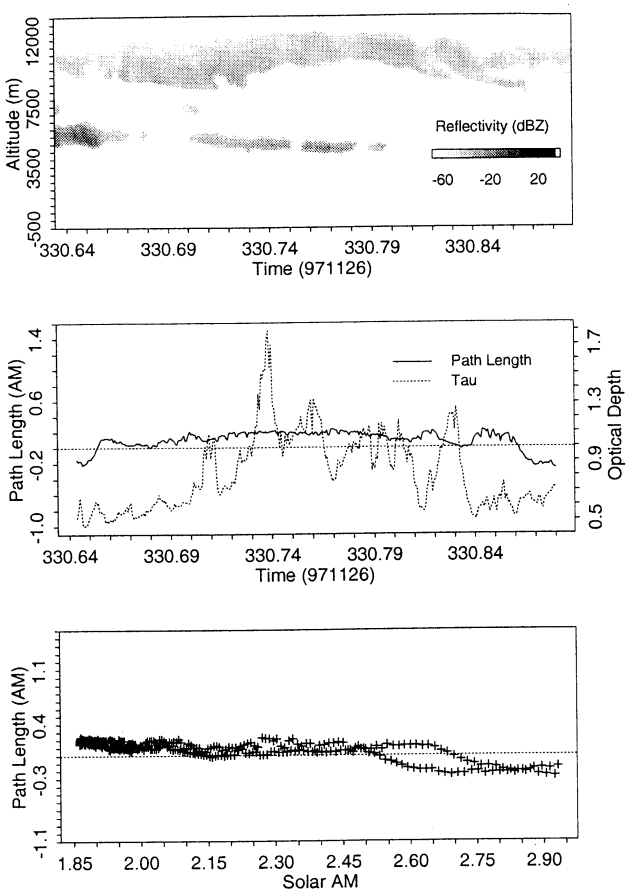


**Figure 3.** Same as in Figure 1 but for November 26, 1997.

the incremental path lengths are more or less constant over several hours with a mean of 1.0 air mass. Both the middle and the bottom panels of Figure 2 exhibit reduced incremental path lengths and even negative incremental path lengths for the greater solar air masses. Since the mean path length inferred by using the oxygen A-band is weighted by the pressure of the lower atmosphere, and scattering aloft can direct more photons vertically downward, negative incremental path lengths are possible at larger solar zenith angles.

### 3.3. Case 3 (Multiple Thin Cloud Layers, November 26, 1997)

Figure 3 shows a case with multiple, thin cloud layers: a thin cirrus cloud layer at 9.6 km with a thin, scattered cloud layer below it at 6.0 km. Cloud optical depths vary from 0.2 to 1.5. The incremental path lengths are approximately 0.2 air masses at local noon and are negative for the greatest solar zenith angles. A small, or negative, incremental path length is a sensitive indicator that the scattering source is a thin cloud aloft. Mean photon path lengths combined with optical depths provide a tool to identify subvisual cirrus that may not be easy to detect with other passive measurements.

## 4. Overcast Thick Clouds

Joint statistics of photon path length and cloud optical depth for cloud optical depths greater than 5 show two different population branches: (1) small variations of path length enhancement over large optical depth ranges and 2) large variances of enhanced photon path lengths, which were illustrated by *Min and Harrison* [1999] for two interesting cases. By assembling relevant instrument measurements, we study four cases to understand various aspects of cloud morphology, radiative smoothing, temporal-spatial variance, and their implications on the photon path length.

Given the nonlinear relationship between irradiance and LWP, there is more insight to be gained by converting irradiance to optical depth. The optical depth is largely determined by the transmittance, and the effective radius plays only the minor role of adjusting the asymmetry factor and single-scattering albedo through narrow ranges. Using MFRSR data alone and assuming $r_e$ to be 8 $\mu$m (without any LWP data used in conjunction with these data), our uncertainty of inferred optical depths of cloud increases by approximately 2-3% above the optimum values obtained using LWP data [*Min and Harrison*, 1996]. In the following discussion cloud optical depths are inferred from MFRSR data alone using the *Min and Harrison* [1996] retrieval algorithm without a LWP constraint.

### 4.1. Case 4 (Thick Single-Layer Cloud, December 8, 1997)

A single-layer, optically thick stratus event occurred on December 8, 1997 (Figure 4). The LWP measured from a MWR and the cloud optical depth inferred from a MFRSR are plotted overlapping each other (Figure 4a). This panel illustrates that the large-scale structures are well-correlated and fluctuate in phase with each other, implying that the variation of effective radius is relatively small. The cloud base height is plotted in Figure 4b, along with the incremental path length, showing that the cloud base height changed gradually from 200 m in the early morning up to 400 m in the late afternoon. The MMCR reflectivity (Figure 4c) illustrates that over the entire period there was a single stratus cloud layer with nearly constant cloud geometric thickness of 500 m. Two relative humidity profiles taken from the BBSS in the afternoon (Figure 4d) confirm that there was only a single cloud layer.

For this low-level stratus, photons transit nearly the full direct-beam path length before encountering the cloud, hence the incremental path length (the total path length minus the direct-beam path length) is essentially the enhanced path length due to clouds. Joint statistics of mean incremental path length and cloud optical depth are shown in Figure 4f. As Figure 4f illustrates, there is a strong correlation of mean incremental path lengths with cloud optical depth apart from slight modulation by cloud base height (Figure 4b). This case is

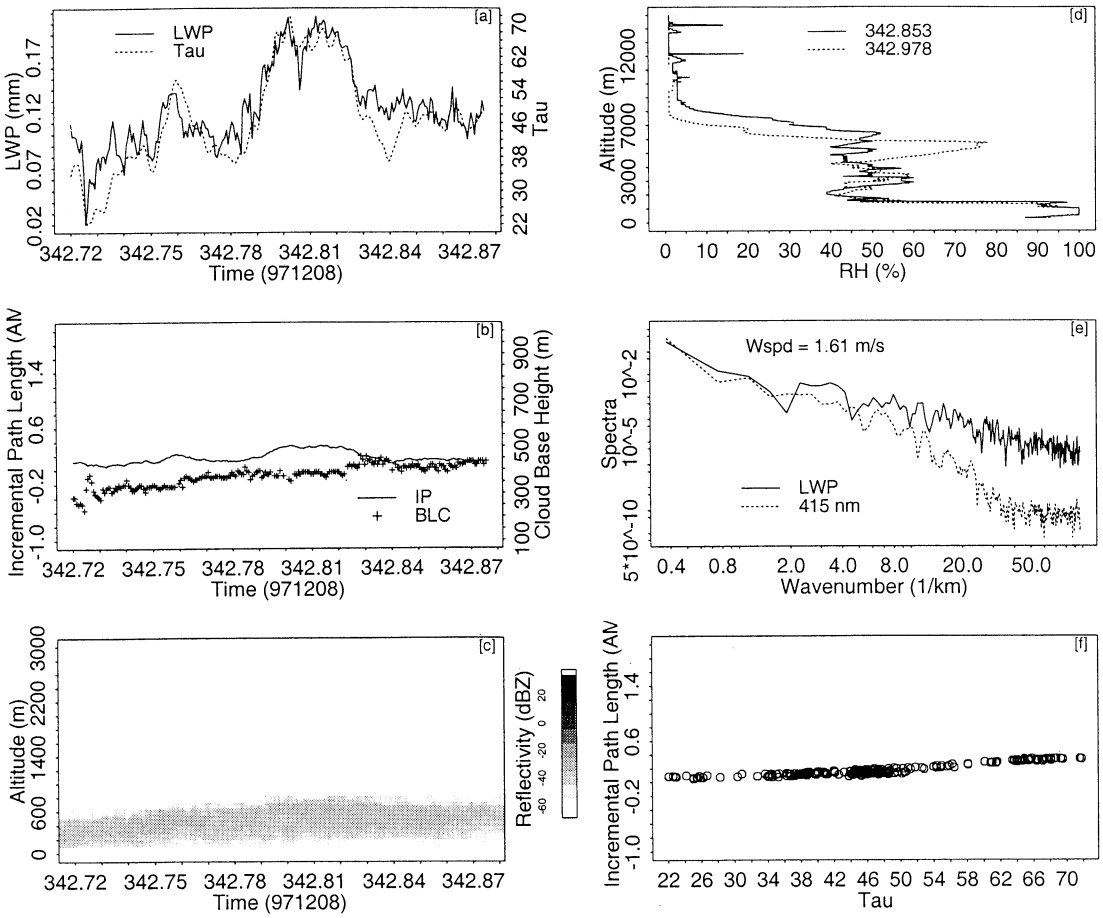


**Figure 4.** A single-layer cloud case on December 8, 1997. (a) Time series of (LWP) and inferred cloud optical depth; (b) times series of incremental path length due to clouds and cloud base height from (BLC); (c) MMCR reflectivity; (d) relative humidity profiles from (BBSS); (e) wavenumber spectra for LWP and transmittance at 415 nm; (f) joint statistics of incremental path length and cloud optical depth.

illustrative of many single-layer cloud cases where the path length scales linearly with optical depth (in this case over the range 20 to 70), thus exhibiting the Brownian diffusion limit for fixed physical depth. In general, the physical depth or altitude (important because the retrieval is pressure-weighted) of the cloud may have correlations with optical depth that would alter the apparent slope; we discuss this possibility more in the next case.

Log-log plots of normalized wavenumber spectra for the LWP and the transmittance at 415 nm from the MFRSR measurements for this case are illustrated in Figure 4e. The mean wind speed at cloud level was 1.61 m/s, allowing us to characterize the wavenumber spectra for the range 0.3 to 80 $km^{-1}$. Except during heavy rain, scattering is negligible at microwave frequencies, so that the LWP of clouds inferred from MWR measurements represents true variations in the cloud fields. The LWP spectrum follows a power-law statistic ($k^{-\beta}$) with a $\beta$ of 1.89, reflecting a statistical scale invariance of clouds over scales from 20 m to several kilometers. The spectrum of the narrowband transmittance at 415 nm illustrates a scale break around 3 $km^{-1}$, indicating a change in the dominant physical process in the radiation field: multiple scattering. At scales larger than the break point the radiation field follows LWP variations in the clouds, while at the smaller scales it shows much smoother behavior with an exponent $\beta$ of 4.09. The smoothness of the radiation field compared to the cloud LWP field is clearly demonstrated in Figure 4a. Simply taking the ratio of LWP and transmittance spectra, we see a nice low-pass filter. This result illustrates that the effect of multiple scattering on the transfer of radiation is to filter out smaller-scale structures leaving the radiance dependent only on the grossest scales [*Stephens*, 1988; *Marshak et al.*, 1995].

### 4.2. Case 5 (Thick Single-Layer Cloud, October 24, 1997)

Another case with a thick single-layer stratus occurred on October 24, 1997 with cloud optical depths up to 120 (Figure 5). The cloud base height shows an-

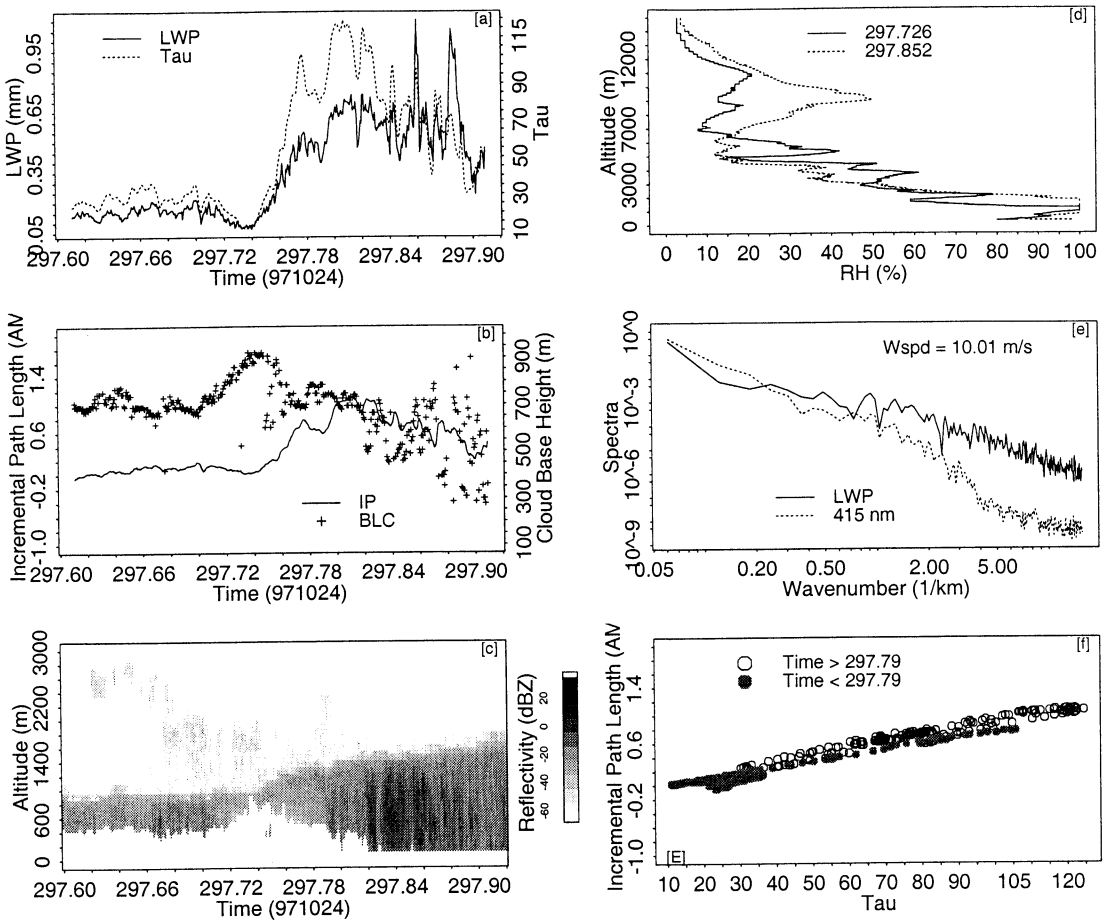


**Figure 5.** Same as Figure 4 but for October 24, 1997.

ticorrelation with cloud LWP and cloud optical depth (Figures 5a, 5b). The MMCR radar reflectivities (Figure 5c) indicate that the cloud boundaries and the geometric thickness of the cloud layer varied with time, with cloud physical depths of 330 m in the morning and of 1000 m in the late afternoon.

Our inferred mean photon path lengths are the pressure- and temperature-weighted path lengths. The enhanced path length due to multiple scattering by clouds is sensitive to the cloud thickness and altitude. To understand the impact of cloud geometry on the enhanced photon path length, we divide the data into two subsets, with a separation at 297.79 Julian time when the cloud boundaries had significant changes, and plot joint statistics of incremental path length and cloud optical depth separately in Figure 5f. As we expected, for constant physical depth the path length scaled linearly with optical depth as for Brownian diffusion; each subset of incremental path length shows a linear relation with optical depth. However, they have different slopes and intercepts: the thicker and lower cloud, the larger slope and intercept.

Note that Figure 5a also shows a strong correlation between cloud LWP and cloud optical depth, except for two large bumps in LWP during the afternoon due to drizzle observed by the Surface Meteorological Observation System (SMOS). The scattering of photons is insensitive to large drizzle droplets, and multiple scattering causes horizontal fluxes that smooth out the small-scale structure seen in the LWP. The exponent $\beta$ of the LWP spectrum is 1.69, and the scale break point of the transmittance spectrum is at $2\,\mathrm{km}^{-1}$ with an exponent $\beta$ of 2.60 for smaller-scale spectra (Figure 5d).

### 4.3. Case 6 (Thick Multiple-Layer Cloud, November 27, 1997)

A thick multiple-layer cloud case took place on November, 27, 1997, indicated by the MMCR radar reflectivity image of Figure 6c. There were three thick cloud layers during this period. The bottom cloud layer varied in thickness with the cloud base height changing from 1.8 km to 0.7 km at 331.77 Julian time (Figure 6b); cloud top height for this layer was constant at 2.0 km. The upper cloud layer was located above 6.0 km with a thickness of about 4.5 km, while the middle cloud layer was located around 4.0 km with varying thickness of 1-2 km. Based on the BBSS sounding, the temperature of the upper layer was less than $-25°$C, while the temperature of the middle layer was greater than $-12°$C;

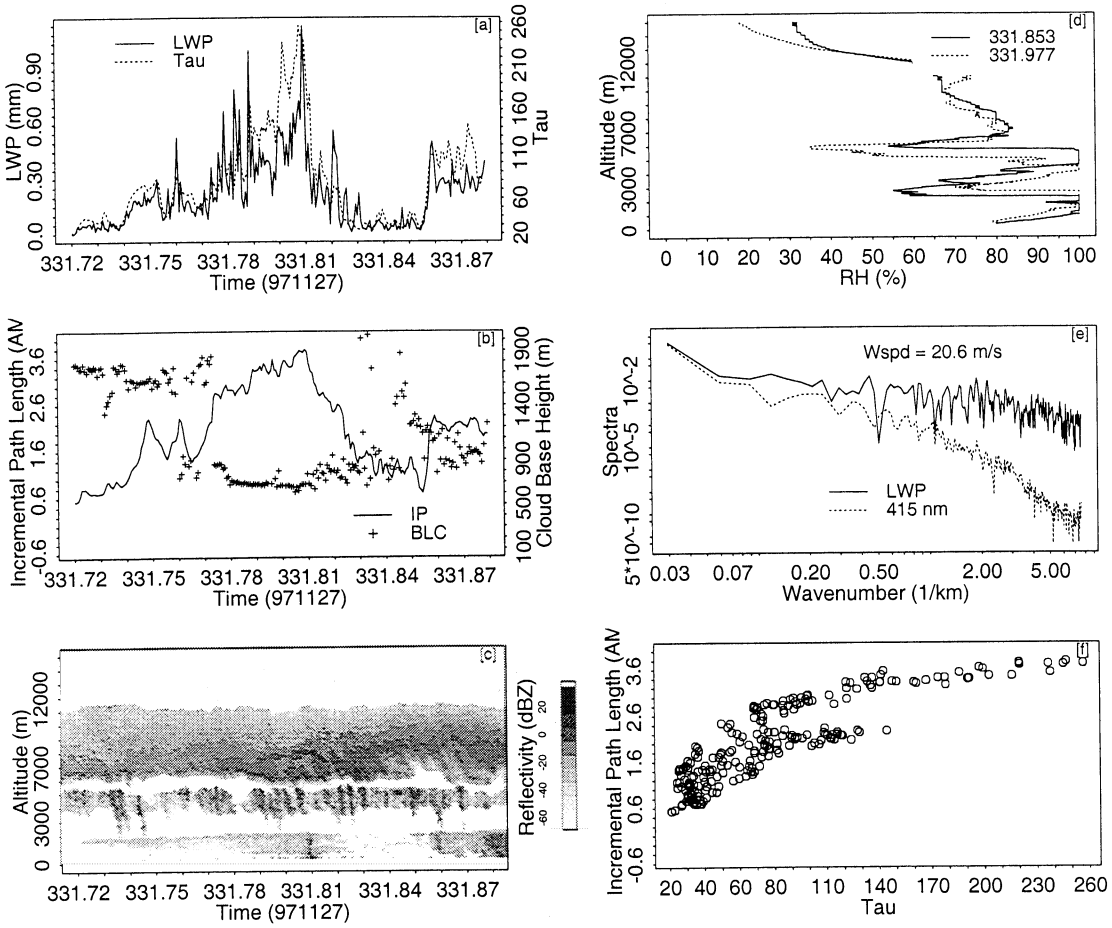


**Figure 6.** Same as Figure 4 but for a multiple cloud layer case on November 27, 1997.

we can treat both lower layers as water clouds for the optical depth retrieval.

The cloud optical depths of this multiple-layer system show smooth behavior and a dramatic range from 10 to 250 (Figure 6a). Cloud optical depths also correlate with cloud LWP in large-scale structure. The scatterplot of mean photon path length and cloud optical depth on the day (Figure 6f) exhibits much greater variance and no longer exhibits the linear relationship seen in single-layer cases. The large incremental path lengths, as well as their variations, occur in part due to multiple photon transits between the layers that do not contribute to the cloud optical depth and also through changes of location and geometric thickness of the cloud layers. Even with strong small-scale fluctuations of LWP, the radiation field is still smooth with an exponent $\beta$ of 4.3 for wavenumbers greater than $0.5\,\mathrm{km}^{-1}$, due to multiple scattering inside clouds and reflections between clouds.

### 4.4. Case 7 (Thick Multiple-Layer Cloud, December 1, 1997)

Another multiple-layer cloud system occurred on December 1, 1997 (Figure 7). The cloud base height of the bottom thick cloud layer varies around 375 m with a cloud physical depth of about 1000 m. As indicated by relative humidity profiles observed in the afternoon, the upper cloud layer was above 5500 m and the cloud temperature was below -25°C, so it may be an ice cloud layer. Unlike the earlier cases, the correlation between cloud LWP and cloud optical depth was weak for the whole period (Figure 7a). However, if the case is divided into two intervals at 335.73 Julian time, the cloud optical depth in each subset exhibits a good correlation with the LWP, indicating that the cloud system underwent a more fundamental change at that time. Our suspicion that the upper ice cloud layer was formed thereafter is confirmed by the MMCR reflectivity image (Figure 7c). The joint statistics of incremental path length and cloud optical depth (Figure 7f) suggest that the linear scaling of path length with optical depth in the morning subset is as expected for a single-layer cloud. For the second subset, however, incremental path lengths are large and exhibit large variability as a result of the multiple-layer cloud system.

Photon transits through this complex multiple-layer cloud system also exhibit the effects of radiative smoothing, as indicated by the wavenumber spectra shown in Figure 7e and by temporal variations shown in Figure 7a. The LWP spectrum follows the power-

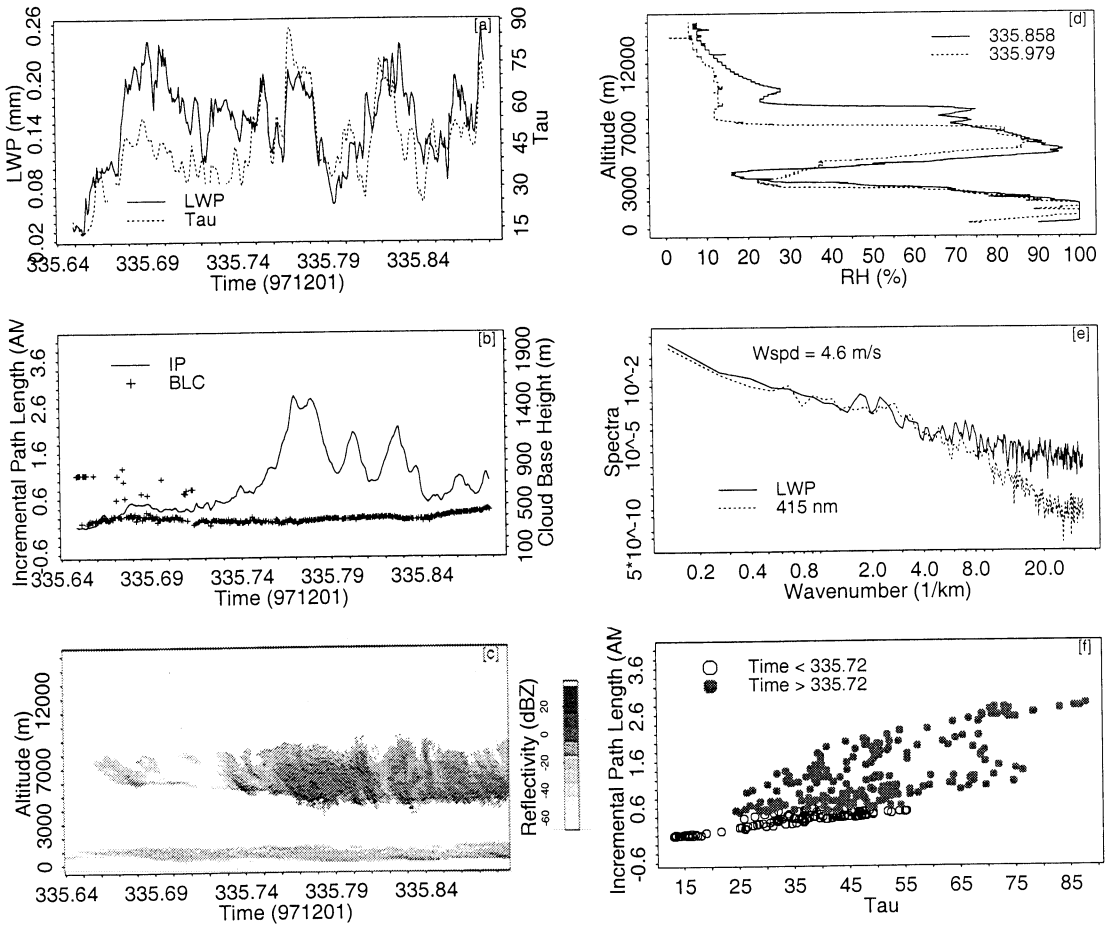


**Figure 7.** Same as Figure 4 but for a multiple cloud layer case on December 1, 1997.

law statistic with an exponent of 1.82 across the entire wavenumber range. The transmittance spectrum, however, shows the scale break at wavenumber $2\text{km}^{-1}$ and has an exponent $\beta$ of 4.6 for smaller scales.

## 5. Discussion

We have analyzed three thin cloud and aerosol cases by comparing the photon path length inferred from $O_2$ A-band spectroscopy with the cloud boundaries and reflectivities obtained from a cloud radar and lidars. Our analyses demonstrate that the photon path length is sensitive to the location of scattering sources, even for optically thin atmospheres. Scattering particles at a high altitude (e.g., thin cirrus clouds) can scatter photons vertically downward to the detector, resulting in reduced or even negative incremental path lengths for diffuse irradiances at greater solar zenith angles. Since the mean path lengths inferred from $O_2$ A-band spectroscopy are weighted by the pressure, aerosols that are loaded predominantly at low levels in the atmosphere scatter photons more horizontally toward the detector, resulting in a significant enhancement of diffuse photon path lengths over the clear-sky direct beam photon path lengths. Note that decrements in the mean photon path length below clear-sky direct beam values identifies subvisual cirrus that may otherwise be undetectable from a sun-photometer measurement alone.

We have presented two single-layer cloud cases, typical of many such systems, where the path length scales linearly with optical depth for fixed physical depth. The wavenumber spectra for these two cases illustrate that the scale break point of the radiation field is proportional to the cloud physical depth, ranging from 200 m to 500 m. This dependence of the scale break on cloud physical depth is characteristic of classical Brownian diffusion [*Marshak et al.*, 1995; *Davis et al.*, 1996]. Therefore photon path lengths occurring in these systems with inhomogeneous single-layer clouds are well represented as Gaussian (being assumed to be in the diffusion approximation) as opposed to having Levy statistics [*Davis and Marshak*, 1998; *Pfeilsticker*, 1999].

Further we have shown two complex multiple-layer cloud systems where the mean incremental path lengths are substantially larger and show great variance of this mean pathlength with time. This is caused by variation in the overlap correlation rather than the inhomogeneity of any individual cloud layer. Photons are temporarily "trapped" between the cloud layers and make multiple transits between the cloud layers in cloud-free air, re-

sulting in a large enhancement of mean photon path length and a greater variance of same. Having photons bounce between cloud layers also enhances horizontal photon transport, resulting in greater radiative smoothing. This point is supported by the wavenumber statistics of the optical depth and cloud LWP time series. In fact, the differences between the optical depth and cloud LWP exponents, i.e., $\beta_{415} - \beta_{\mathrm{LWP}}$, are 3.06 and 2.78 for the two multiple-layer cloud cases and 2.00 and 0.91 for the two single-layer cloud cases.

Scale-by-scale statistical analysis shows that there is a scale break-point, or "radiative smoothing scale," that separates two physically distinct regimes. For scales larger than the breakpoint, the LWP and radiation fields have the same power spectrum, while for smaller scales, the radiation field has a larger spectral exponent than that of the LWP field. The small-scale regime is dominated radiatively by a horizontal transport process as a result of multiple scattering, so the radiation fields are much smoother than the LWP [*Marshak et al.*, 1995]. Overlapped plots of time series of LWP and cloud optical depth illustrate that the fluctuations in the radiation fields vary in phase with the LWP fields at scales larger than the breakpoint.

*Marshak et al.* [1995] argued that the independent pixel approximation (IPA), for which each pixel is treated as a plane-parallel layer, can be applied to infer optical depth from measured radiance for scales larger than the "radiative smoothing scale." For smaller scales the IPA fields should be corrected by convolution with some probability density function to generate smoother fields. In general, various instruments have different sampling rates and observational geometries, and large-scale fluxes and transmittances are the important quantities for cloud overlap schemes and sub-grid-scale parameterizations in GCMs. Hence it is critical to understand the effects of spatial-temporal variability on radiation parameter retrievals from multiple instrument measurements, particularly for combining radiation measurements and active or passive observations that are confined to relatively narrow vertical columns through clouds.

A common practice is to combine radiation measurements and the LWP (and water vapor path) to infer the cloud optical depth and effective radius. An important question becomes the optimal spatial (or temporal) scale at which to combine the two measurements. We apply a running mean on the LWP, equivalently a low-pass filter, to smooth out the smaller-scale structures, and then correlate it with our inferred cloud optical depth to test the optimal averaging time. The correlation coefficients as a function of averaging time for the case of December 8, 1997 (Figure 8), illustrates that the optimal averaging time is about 9 min. With the wind speed indicated in Figure 4, the corresponding optimal scale of spatial averaging for the LWP is about 3 times the "radiative smoothing scale." The optimal averaging time for each individual case changes with the advection. However, the scaling factor of 3 is more or less the same for all the cases we analyzed. As Figure 8 also shows, using linear or geometric (logarithm) means makes little difference in estimating the optimal scale of spatial averaging.

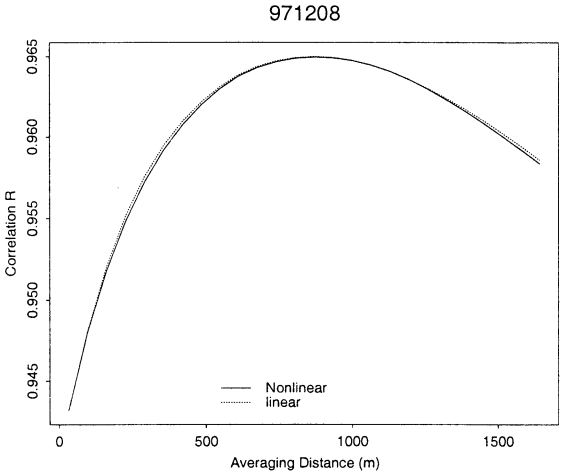


**Figure 8.** Correlation coefficients between the cloud LWP and the optical depth for the case of December 8, 1997.

## 6. Summary

We have studied photon path length, cloud morphology and inhomogeneity, radiative smoothing, and their implications under various conditions using high time resolution data streams from various colocated instruments at the ARM SGP site. Our extensive case studies show that observation of mean photon path length allows some classification of cloud and sky scenes that cannot be done readily by other passive remote sensing techniques: the identification of multiple layer clouds, and isolated subvisual cirrus.

The climatology of these joint statistics of mean photon path length and optical depth can be used to test the representativeness of GCM cloud-diagnostic schemes. And these joint statistics, in conjunction with radar and lidar measurements, may provide a powerful remote sensing technique to improve our understanding of cloud layer geometric properties on relevant optical properties.

Scale-by-scale statistical analysis of cloud LWP and cloud optical depth illustrates that the effect of multiple scattering on the transfer of radiation through a heterogeneous atmosphere is to filter out smaller scale structure leaving the radiance dependent only on the large scales. For large-scale fluxes and transmittances the optimal spatial scale of cloud LWP measurements, in conjunction with radiation measurements, is about 3 times the "radiative smoothing scale," depending on the physical thickness of the cloud system.

**Acknowledgments.** This research was supported by the Environmental Sciences Division of U.S. Department of Energy under grants DE-FG02-90ER61072 and DE-FG02-90ER61071 as part of the Atmospheric Radiation Measurement Program and National Science Fundation under grant ATM-9973701. Data were obtained from the Atmospheric Radiation Measurement (ARM) Program sponsored by the U.S. Department of Energy, Office of Energy Research, Office of Health and Environmental Research, Environmental Sciences Division.

## References

Cahalan, R. F., and J. B. Snider, Marine stratocumulus structure, *Remote Sens. Environ., 28,* 98-107, 1989.

Cahalan, R. F., W. Ridgway, W. J. Wiscombe, T. L. Bell, and J. B. Snider, The albedo of fractal stratocumulus clouds, *J. Atmos. Sci., 51*, 2434, 1994a.

Cahalan, R. F., W. Ridgway, W. J. Wiscombe, S. Gollmer, and J. B. Harshvardan, Independent pixel and Monte Carlo estimates of stratocumulus albedo, *J. Atmos. Sci., 51*, 3776, 1994b.

Davis A., A. Marshak, W. Wiscombe, and R. Cahanlan, Scale invariance in liquid water distributions in marine stratocumulus, part I, Spectral properties and stationarity issues, *J. Atmos. Sci., 53,* 1538-1558, 1996.

Davis A., A. Marshak, R. F. Cahalan, and W. J. Wiscombe, The Landsat scale break in stratocumulus as a three-dimensional radiative transfer effect: Implications for cloud remote sensing, *J. Atmos. Sci., 54,* 241-260, 1997.

Davis A., and A. Marshak, Levy kinetics in slab geometry scaling of transmission probability, in *Fractal Frontiers*, edited by M. M. Novak and T. G. Dewey, pp.63-72, World Sci., Singapore, 1998.

Grechko, Y. I., V. I. Dianov-Klokov, and I. P. Malkov, Aircraft measurements of photon paths in reflection of transmission of light by clouds in 0.76-micron oxygen band, *Izv. Atmos. Oceanic Phys., 9,* 471-485, 1973.

Harrison, L., and Q.-L., Min, Photon path length Distributions in cloudy atmospheres from ground-based high-resolution $O_2$ A-band spectroscopy, in *IRS'96: Current Problems in Atmospheric Radiation,* edited by W. L. Smith and K. Stamnes, A Deepak, Hampton, Va., 1997.

Harrison, L. C., M. Beauharnois, J. Berndt, P. Kierdron, J. Michalsky, and Q.-L. Min, The rotating shadowband spectroradiometer (RSS) at the Southern Great Plains (SGP), *Geophys. Res. Lett., 26,* 1715-1718, 1999.

Heidinger, A., and G. L. Stephens, Molecular line absorption in a scattering atmosphere, 2, Retrieval of particle properties, *J. Atmos. Sci., 57*, 1615-1634, 2000.

Lovejoy, S., D. Schertzer, P. Silas, Y. Tessier, and D. Lavallee, The unified scaling model of atmospheric dynamics and systematic analysis of scale invariance in cloud radiances, *Ann. Geophys., 11*, 119-127, 1993.

Marshak, A., A. Davis, R. F. Cahalan, and W. J. Wiscombe, Radiative smoothing in fractal cloouds, *J. Geophys. Res., 100*, 26,247 -26,261, 1995.

Marshak, A., A. Davis, W. J. Wiscombe, and R. F. Cahalan, Scale invariance in liquid water distributions in marine stratocumulus, part II, Multifractal properties and intermittency issues, *J. Atmos. Sci., 54,* 1423-1444, 1997.

Min, Q.-L., and L. C. Harrison, Cloud properties derived from surface MFRSR measurements and comparison with GOES results at the ARM SGP site, *Geophys. Res. Lett., 23*, 1641, 1996.

Min, Q.-L., and L. C. Harrison, Joint statistics of photon path length and cloud optical depth, *Geophys. Res. Lett., 26*, 1425-1428, 1999.

Pfeilsticker, K., F. Erle, H. Veitel, and U. Platt, First geometrical path lengths probability density function derivation of the skylight from high resolution oxygen A-band, 1, Measurement technique, atmospheric observations and model calculations *J. Geophys. Res. 103*, 11483, 1998

Pfeilsticker, K., First geometrical path length probability density function derivation of the skylight from high resolution oxygen A-band, 2, Derivation of the Levy index for the skylight transmitted by midaltitude clouds, *J. Geophys. Res., 104*, 4101-4116, 1999.

Stephens, G., The transfer of radiation through vertically nonuniform Sc clouds, *Contrib. Phys. Atmos., 49.*, 237-253, 1976.

Stephens, G. L., Radiative transfer through arbitrarily shaped optical media, I, A general method of solution, *J. Atmos. Sci., 45,* 1818-1836, 1988a.

Stephens, G. L., Radiative transfer through arbitrarily shaped optical media, II, Group theory and simple closures, *J. Atmos. Sci., 45,* 1837-1848, 1988b.

Stephens, G. L., and A. Heidinger, Molecular line absorption in a scattering atmosphere: 1 Theory, *J. Atmos. Sci., 57,* 1599-1614, 2000.

Van de Hulst, H. C., Multiple light scattering, Academic, San Diego, Calif. 1980.

Veitel, H., O. Funk, C. Kruz, U. Platt, and K. Pfeilsticker, Geometrical path length probability density functions of the skylight transmitted by midlatitude cloudy skies: Some case studies, *Geophys. Res. Lett., 25*, 3355, 1998.

Welch, R. M., and B. A. Wielicki, Cumulus cloud properties derived using Landsat data, *J. Clim. Appl. Meteorol., 25*, 261-276, 1986.

Q. Min and L. C. Harrison, Atmospheric Sciences Research Center, State University of New York at Albany, 251 Fuller Road, Albany, NY 12203. min@asrc.cestm.albany.edu

E. E. Clothiaux, Department of Meteorology, The Pennsylvania State University, University Park, PA 16802

(Received December 31, 1999; revised July 18, 2000; accepted August 2, 2000.)